Mandelamide Hydrolase from *Pseudomonas putida*: Characterization of a New Member of the Amidase Signature Family†

Kota N. Gopalakrishna,‡ Betty H. Stewart,§ Malea M. Kneen, Adriano D. Andricopulo,|| George L. Kenyon, and Michael J. McLeish*

College of Pharmacy, University of Michigan, Ann Arbor, Michigan 48109-1065

Received January 12, 2004; Revised Manuscript Received April 14, 2004

ABSTRACT: A recently discovered enzyme in the mandelate pathway of *Pseudomonas putida*, mandelamide hydrolase (MAH), catalyzes the hydrolysis of mandelamide to mandelic acid and ammonia. Sequence analysis suggests that MAH is a member of the amidase signature family, which is widespread in nature and contains a novel Ser-*cis*-Ser-Lys catalytic triad. Here we report the expression in *Escherichia coli*, purification, and characterization of both wild-type and His_6-tagged MAH. The recombinant enzyme was stable, exhibited a pH optimum of 7.8, and was able to hydrolyze both enantiomers of mandelamide with little enantiospecificity. The His-tagged variant showed no significant change in kinetic constants. Phenylacetamide was found to be the best substrate, with changes in chain length or replacement of the phenyl group producing greatly decreased values of k_{cat}/K_m. As with another member of this family, fatty acid amide hydrolase, MAH has the uncommon ability to hydrolyze esters and amides at similar rates. MAH is even more unusual in that it will only hydrolyze esters and amides with little steric bulk. Ethyl and larger esters and *N*-ethyl and larger amides are not substrates, suggesting that the MAH active site is very sterically hindered. Mutation of each residue in the putative catalytic triad to alanine resulted in total loss of activity for S204A and K100A, while S180A exhibited a 1500-fold decrease in k_{cat} and significant increases in K_m values. Overall, the MAH data are similar to those of fatty acid amide hydrolase and support the suggestion that there are two distinct subgroups within the amidase signature family.

A number of pseudomonads are able to use one or both of the enantiomers of mandelic acid as their sole carbon source (*1*). This ability is provided by the enzymes in the mandelate metabolic pathway which facilitate the conversion of both (*R*)- and (*S*)-mandelate to benzoate, which is subsequently converted to acetyl-CoA and succinyl-CoA by the enzymes of the β-ketoadipate pathway (Figure 1). Initial studies indicated that the genes for the mandelate pathway of *Pseudomonas putida* (ATCC 12633) were all closely clustered on the chromosome (*2*, *3*). Subsequently, the genes were found to reside on a single 10.5 kb restriction fragment (*4*), and three of the genes, those for mandelate racemase (*mdl*A), (*S*)-mandelate dehydrogenase (*mdl*B), and benzoylformate decarboxylase (*mdl*C), were found to be arranged in an operon (*4*).

Further sequencing of the restriction fragment encoding the enzymes of the mandelate pathway has revealed three more open reading frames which have been denoted *mdl*D, *mdl*X, and *mdl*Y (*5*). The *mdl*D gene product was shown to be a $NAD(P)^+$-dependent benzaldehyde dehydrogenase, while the deduced amino acid sequence of the *mdl*X gene product suggested that it encodes a transcriptional regulatory protein (*5*). The deduced amino acid sequence of the *mdl*Y gene product was considerably homologous with the sequences of a number of bacterial amide hydrolases (amidases, EC 3.5.1.4). This homology, together with the location of the *mdl*Y gene within the mandelate pathway gene cluster, suggested that *mdl*Y encodes a mandelamide hydrolase. Subsequently, it was demonstrated that the *mdl*Y gene product was indeed able to convert both (*R*)- and (*S*)-mandelamide to mandelic acid (*5*).

Mandelamide hydrolase appears to be a member of a large group of enzymes which have been termed the amidase signature (AS)[1] family (*6*, *7*). The family is characterized by the presence of a highly conserved serine- and glycine-rich stretch of approximately 50 amino acids (Figure 2). Members of this family have been identified in more than 90 different organisms (*8*), including archaea, eubacteria, fungi, nematodes, plants, insects, birds, and mammals (*9*). Although the biochemical function of the amidases is simply the hydrolysis of the amide bond ($RCO-NH_2$), the biological consequences of the reaction are diverse. These include carbon−nitrogen metabolism in prokaryotes and eukaryotes (*10*, *11*), formation of indole-3-acetic acid in pathogenic plant bacteria (*12*), degradation of neuromodulatory fatty acid amides in mammals (*13*, *14*), and formation of Gln-tRNAGln

† This research was supported, in part, by U.S. Public Health Service Grant GM-40570 (to G.L.K.).

* To whom correspondence should be addressed. Telephone: (734) 615-1787. Fax: (734) 615-3079. E-mail: mcleish@umich.edu.

‡ Current address: Medical College of Georgia, Augusta, GA 30912.

§ Current address: Austin College, Sherman, TX 75090.

|| Current address: Center for Structural Molecular Biotechnology, Universidade de São Paulo, São Paulo, Brazil.

[1] Abbreviations: AS, amidase signature; MAH, mandelamide hydrolase; FAAH, fatty acid amide hydrolase; MAE2, malonamidase E2; PAM, peptide amidase; PMSF, phenylmethanesulfonyl fluoride; DFP, diisopropyl fluorophosphate; IPTG, isopropyl β-D-thiogalactopyranoside; SDS−PAGE, sodium dodecyl sulfate−polyacrylamide gel electrophoresis; WT, wild-type; CD, circular dichroism.

10.1021/bi049907q CCC: $27.50
Published on Web 05/25/2004

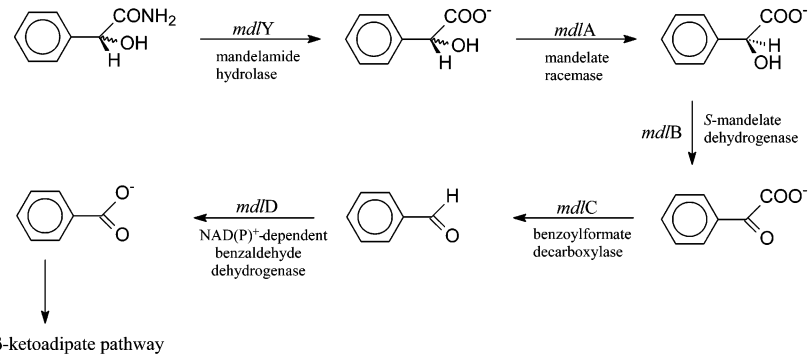

FIGURE 1: Mandelate metabolic pathway of *P. putida*, including mandelamide hydrolase (*5*). The genes for benzoylformate decarboxylase, (*S*)-mandelate dehydrogenase, and mandelate racemase are arranged in an operon (*mdl*CBA) and are transcribed away from *mdl*D and *mdl*Y.

MAH	176	IA**GGSSSG**SG TAVGALLIPA ALGTDTGG**S**V
MAE2	127	SP**GGSSSG**SA AAVGAGMIPL ALGTQTGG**S**V
FAAH	213	SP**GGSGG**EG ALIGSGGSPL GLGTDIGG**S**I
ESTA8	148	NS**GGSGG**SA SAVAAGIVPI AGAGDGGG**S**I
IAH	145	IP**GGSGG**VA AAVAGRLMLG GVGTDTGA**S**V
ESAM	145	TP**GGSGG**TA AALAAGLIFA GMGTDTGG**S**I
AMID	167	EA**GGSGG**SA ALVANGDVDF AIGGDQGG**S**I
PYRA	149	IA**GGSGG**SA AAVAAGLVPL TLGSDTNG**S**I
ACET	200	SC**GGSGG**EG AIVGIRGGII GVGTDIGG**S**I
6AHH	136	SV**GGSGG**SG AAVAAALSPV AHGNDAAG**S**V
VD3H	221	TP**GGSGG**EG ALIAGGGSLL GIGSDVAG**S**I
UREA	156	VS**GGSSAG**SA SVVARGIVPI ALGTDTAG**S**G
GATA	150	IP**GGSGG**SS AALAAFQAPL AIGTDTGG**S**I
PAM	198	SP**CGSSSG**SA VAVAANLASV AIGTETDG**S**I

FIGURE 2: Multiple-sequence alignment of the region encompassing the amidase signature sequence of enzymes identified as having sequences homologous to that of mandelamide hydrolase. The enzymes were identified using a Blast search (*71*) of the protein database. The top-scoring individual for each enzyme was used for this alignment: MAH, mandelamide hydrolase, *P. putida* (gi27762473); MAE2, malonamidase E2, *B. japonicum* (gi4102573); FAAH, fatty acid amide hydrolase, *Homo sapiens* (gi6225310); EstA8, esterase A8, *Acinetobacter* sp. (*39*); IAH, indoleacetamide hydrolase, *Agrobacterium rhizogenes* (gi1170450); ESAM, enantiomer specific amidase, *Rhodococcus* sp. (gi98837); AMID, amidase, *R. erythropolis* (gi113712); PYRA, pyrazinamidase/nicotinamidase, *Caulobacter crescentus* (gi13424188); ACET, acetamidase, *Aspergillus ustus* (gi13569683); 6AHH, 6-aminohexanoate-cyclic-dimer hydrolase, *Flavobacterium* sp. K172 (gi129000); VD3H, vitamin D_3 hydroxylase-associated protein, *Gallus gallus* (gi2492838); UREA, urea amidolyase, *Saccharomyces cerevisiae* (gi6319685); GATA, glutamyl-tRNA amidotransferase subunit A, *Streptomyces coelicolor* (gi6225417); PAM, peptide amidase, *Stenotrophomonas maltophilia* (gi19744118).

by transfer of ammonia from glutamine (*15*, *16*). Surprisingly, given the widespread occurrence of the amidases, it has only been recently that any structural or mechanistic studies of this class of enzymes have been undertaken. The most detailed studies are on the mammalian enzyme fatty acid amide hydrolase (FAAH) which is responsible for the catabolism of a family of endogenous signaling lipids (*13*, *14*). Since this enzyme affects endogenous pain and sleep−wake systems, it has become a target for pharmaceutical development (*17*, *18*) and, consequently, more concentrated investigation (*9*, *19*−*21*). The initial studies showed that the amidase signature family operated by an unusual catalytic mechanism, employing a combination of serine and lysine residues possibly in the form of a dyad (*9*).

To date, X-ray structures of three members of this family have been reported (*8*, *22*−*24*). The overall folds were all similar and contain a mixed β-sheet comprising 10 strands. Together, they form a distinct family in the SCOP (structural characterization of proteins) database (*25*). The first structure to be reported, that of malonamidase E2 (MAE2) from *Bradyrhizobium japonicum*, revealed an unusual Ser-*cis*-Ser-Lys catalytic triad (*8*, *22*). When the X-ray structure of FAAH became available, it too revealed a nearly superimposable conformation of catalytic residues (*23*), although the substrate binding pockets were significantly different from those of MAE2. The X-ray structure of the third member of the AS family, a peptide amidase (PAM) from *Stenotrophomonas maltophilia*, also showed the presence of the now familiar Ser-*cis*-Ser-Lys catalytic triad (*24*). As with the other two structures, the residues involved in substrate recognition were not conserved, thus emphasizing the functional diversity of this class of enzymes.

Although the positions of the proposed catalytic residues are superimposable with root-mean-square deviations of less than 0.32 Å (*8*), the three enzymes did exhibit some catalytic differences. PAM, for example, did not react with serine reagents such as diisopropyl fluorophosphate (DFP) and phenylmethanesulfonyl fluoride (PMSF) (*24*). In that respect, it was similar to MAE2 which was not inhibited by PMSF (*26*) as well as an amidase from *Rhodococcus rhodochrous* J1 which was insensitive to both DFP and PMSF (*27*). Conversely, FAAH was inhibited by both serine reagents (*28*) as well as halophosphonate affinity labels (*19*). As a result, it has been suggested that there may be at least two groups of enzymes within the AS family with each employing different catalytic mechanisms (*24*). It was of interest to us to confirm that mandelamide hydrolase was indeed a member of the AS family and to identify the group, if any, to which it belongs. Here, we report the characterization of MAH, including studies on substrate specificity, reaction with potential affinity labels, and mutagenesis of putative catalytic residues.

EXPERIMENTAL PROCEDURES

Materials. The mandelamide hydrolase expression vector, pET17mdlY, was available from a previous study (*5*). Methylamine dehydrogenase was a kind gift of V. L. Davidson (University of Mississippi Medical Center, Jackson, MS). Restriction enzymes, ligases, DNA polymerase, and other molecular biology reagents were obtained from New

England Biolabs, Promega, Stratagene, or Novagen. PCR, mutagenesis, and sequencing primers were obtained from the DNA Synthesis Core Facility (University of Michigan). Stearamide and lauramide (dodecanamide) were from TCI America. Unless otherwise stated, all other chemicals and reagents were purchased from either Fisher Scientific or Sigma-Aldrich and were of the highest available purity.

Preparation of His_6-Tagged Mandelamide Hydrolase. Using pET17mdlY as the template, *Pfu* DNA polymerase and the QuikChange site-directed mutagenesis kit (Stratagene) were employed to introduce an *Xho*I restriction site at the C-terminus of the *mdl*Y gene. The sequence of the forward primer used for the mutagenesis, with the *Xho*I site underlined and the lowercase letters indicating a base change from the sequence of the wild type, is 5′-GCAAAATTTC-CcTcgAGCACTGCCGATCCCAAGTCGG-3′. The resultant plasmid was digested with *Nde*I and *Xho*I and the 1.6 kb fragment ligated into *Nde*I- and *Xho*I-digested pET24b, resulting in a plasmid, denoted pET24MAH-his. The fidelity of the mutagenesis was confirmed by sequencing. The vector used for protein expression, pET17MAH-his, was prepared by ligation of a *Mfe*I−*Blp*I fragment of pET24MAH-his, containing MAH-his, into *Mfe*I- and *Blp*I-digested pET17mdlY.

Preparation of His_6-Tagged Mandelamide Hydrolase Mutants. Mutagenesis reactions were carried out by using *Pfu* DNA polymerase and the QuikChange site-directed mutagenesis kit (Stratagene), using pET17MAH-his as the DNA template. The forward primers are given with the mutated codons underlined and the lowercase letters indicating a base change from the sequence of the wild type: 5′-GTACCGATCGCaGTAgctGACAACATCCAGGT-GGTTG-3′ for K100A, 5′-CGCGGGCGGGgCGTCCTCTG-GCAGCGGTACTG-3′ for S180A, 5′-CGCGGGCGGGTCG-gCCTCTGGCAGCGGTACTG-3′ for S181A, and 5′-CCGA-TACAGGTGGcgCcGTTCGACAGCCTGGT-3′ for S204A.

These mutations introduced additional *Alw*NI (K100A), *Bsa*HI (S180A), *Bsr*BI (S181A), and *Bsa*HI (S204A) restriction sites. After treatment with *Dpn*I which removed template DNA, the PCR product was transformed into *Escherichia coli* strain JM109. Single colonies were picked, and the DNA was isolated and screened for the presence of the desired mutation by digestion with the appropriate restriction enzyme. The presence of the mutation and fidelity of the mutagenesis were confirmed by sequencing.

Expression and Purification of Wild-Type Mandelamide Hydrolase. Mandelamide hydrolase was purified from *E. coli* strain BL21(DE3)pLysS (Novagen) which had been transformed with pET17mdlY. A freshly transformed, single colony was selected and used to inoculate 50 mL of Luria broth containing 50 μg/mL ampicillin and 25 μg/mL chloramphenicol. This culture was grown overnight at 37 °C and used to inoculate 1 L of fresh medium. The fresh culture was grown at 37 °C until the OD_{600} reached ∼0.6−0.8. The cells were cooled to 28 °C, and protein expression was induced by the addition of 0.4 mM isopropyl β-D-thiogalactopyranoside (IPTG). The cells were grown for an additional 6 h at 28 °C prior to being harvested by centrifugation at 4 °C. The cell pellet was washed and resuspended in 50 mM phosphate buffer (pH 7.0) containing 1 mM EDTA. Cell lysis was achieved by sonication, and the lysate was cleared by centrifugation at 15000*g* and 4 °C for 30 min.

The clarified cell free extract was subjected to ammonium sulfate fractionation with the fraction precipitating between 0 and 40% saturation being collected and dissolved in 50 mM potassium phosphate buffer (pH 7.0) containing 1 mM EDTA. Following dialysis against the same buffer at 4 °C, the protein was subjected to size-exclusion chromatography on Sephacryl S-200 column which had been equilibrated with 20 mM potassium phosphate buffer (pH 6.0) and 1 mM EDTA (buffer A). Fractions containing MAH activity were pooled, concentrated, and applied to a HiPrep Q anion-exchange column which was attached to an Akta-FPLC system (Amersham Pharmacia Biotech). The column was washed with buffer A until there was no further elution of the protein. MAH was eluted with a linear gradient of NaCl (from 0 to 0.5 M) in buffer A with activity eluting at ∼250 mM NaCl. Fractions containing activity were dialyzed against 100 mM potassium phosphate buffer (pH 7.8) containing 1 mM EDTA (buffer B). In a final step, the enzyme solution was applied to HiTrap Q column (5 mL) equilibrated with buffer B. A linear gradient from 0 to 0.5 M NaCl in buffer B was used to elute the purified enzyme. Fractions containing MAH were pooled, concentrated, and stored in aliquots at −20 °C.

Expression and Purification of Hexahistidine-Tagged Mandelamide Hydrolase Variants. Following the transformation of the appropriate expression vector into *E. coli* strain BL21(DE3)pLysS, a single colony was selected. After inoculation and growth as described for wild-type MAH, protein expression was induced by the addition of IPTG (0.4 mM). Again the cells were grown at 28 °C for 6 h prior to harvest and resuspension in 20 mM phosphate buffer (pH 7.0). After sonication and centrifugation, the cleared lysate was loaded onto a Sepharose CL-6B Ni−nitriloacetic acid (NTA) column (Qiagen) which had been equilibrated in 20 mM phosphate (pH 7.0) containing 20 mM imidazole. The column was washed with the same buffer and again with 20 mM phosphate (pH 7.0) and 50 mM imidazole. Finally, the MAH-his was eluted with 250 mM imidazole in 20 mM phosphate (pH 7.0). Following dialysis against buffer B, the fractions containing MAH-his were concentrated and loaded onto a Sephacryl S-200 gel filtration column which had been equilibrated with the same buffer. The fractions containing the highly purified MAH-his variants were concentrated and stored at −20 °C.

Mass Spectrometry. Electrospray mass spectrometry was performed on a Finnigan LCQ mass spectrometer interfaced with a Finnigan Surveyor HPLC system. The HPLC system was equipped with a Vydac C_{18} reversed phase column (4.6 mm × 250 mm), and the mobile phase was composed of 0.1% acetic acid, 0.02% trifluoroacetic acid, and acetonitrile. MAH was eluted with a linear gradient of 0 to 90% acetonitrile.

Circular Dichroism Spectropolarimetry. Protein samples for far-UV circular dichroism (CD) were exchanged into 100 mM potassium phosphate buffer (pH 7.8) and 1 mM EDTA. Far-UV CD spectra of protein samples (0.2−0.3 mg/mL) were recorded at 20 °C, in triplicate, at a scanning speed of 20 nm/min in a 1.00 mm cell using a JASCO J-810 spectropolarimeter.

Chemical Syntheses. ^{1}H NMR and ^{13}C NMR spectra were recorded on a Bruker DPX300 spectrometer using tetramethylsilane as an internal standard. Chemical shifts are

reported in parts per million (δ). High-resolution mass spectra (HRMS) were recorded on a Micromass Corp VG 70-250-S spectrometer at the University of Michigan Mass Spectrometry Laboratory. Chemical ionization (CI) mass spectra were obtained using NH_3 as the reagent gas. Melting points were determined in a Fisher Scientific melting point apparatus and are uncorrected.

(*R*)- and (*S*)-mandelamide were prepared from the corresponding carboxylic acid, via the acetonide, in a manner similar to that described by Audrieth and Sveda (*29*).

(*R*)-(−)-Mandelamide was obtained as white crystals (EtOH) in 49% yield [based upon (*R*)-(−)-mandelic acid]: mp 124−126 °C [lit. (*30*) 123−124 °C]; ^{1}H NMR (300 MHz, DMSO) δ 4.83 (s, 1H, CH), 6.01 (s, 1H, OH), 7.18 (s, 2H, NH_2), 7.43 (m, 5H, ArH); ^{13}C NMR (75 MHz, DMSO-d_6) δ 175.41, 142.25, 128.73, 128.15, 127.35, 74.30; HRMS CI (NH_3) [M + H] calcd for $C_8H_{10}NO_2$ 152.0711, found 152.0709.

(*S*)-(+)-Mandelamide was also obtained as white crystals (EtOH) in 54% yield [based upon (*S*)-(+)-mandelic acid]: mp 125−126 °C [lit. (*31*) 120−121 °C]; ^{1}H NMR (300 MHz, DMSO) δ 4.83 (s, 1H, CH), 6.01 (s, 1H, OH), 7.18 (s, 2H, NH_2), 7.43 (m, 5H, ArH); ^{13}C NMR (75 MHz, DMSO-d_6) δ 175.42, 142.25, 128.73, 128.15, 127.35, 74.30; HRMS CI (NH_3) [M + H] calcd for $C_8H_{10}NO_2$ 152.0711, found 152.0707.

3-Phenyl-1,1,1-trifluoro-2-propanone was prepared using the procedure of Bovin (*32*). An additional distillation (bp 42−43 °C, 1 mmHg) was required to afford the highly pure trifluoromethyl ketone as a colorless oil (1.6 g, 43%): ^{1}H NMR (500 MHz, $CDCl_3$) δ 7.42−7.38 (m, 3H), 7.28−7.25 (m, 2H), 4.05 (s, 2H); ^{13}C NMR (125 MHz, $CDCl_3$) δ 189.68, 189.40, 189.12, 188.84, 119.71, 117.38, 115.43, 112.73, 43.40; HRMS (EI, 70 eV) calcd for $C_9H_7F_3O$ 188.0449, found 188.0451.

3-Phenyl-1-chloro-2-propanone was synthesized using a modification of the procedure of McPhee and Klingsberg (*33*). Phenylacetyl chloride (3.1 g, 2.65 mL, 20 mmol) was added dropwise to a stirred solution of diazomethane (1.6 g, 40 mmol) in dry ether (250 mL) at 0 °C. The reaction mixture was stirred for 3 h at room temperature before being saturated with dry hydrogen chloride gas at the ice bath temperature. The mixture was washed with a solution of water and sodium bicarbonate. The aqueous layer was extracted with ether (2 × 25 mL). The organic phases were combined, washed with brine, and dried over anhydrous $MgSO_4$. The solvent was removed under reduced pressure and the residue purified by flash column chromatography (silica gel, eluting with hexanes and ethyl acetate) to afford a yellowish oil. This was distilled [bp 110−111 °C, 10 mmHg; lit. (*33*) bp 133−135 °C, 19 mmHg] to yield the chloromethyl ketone as a colorless oil (1.51 g, 45%): ^{1}H NMR (500 MHz, $CDCl_3$) δ 7.40−7.37 (m, 3H), 7.26−7.23 (m, 2H), 4.73 (s, 2H), 4.11 (s, 2H); ^{13}C NMR (125 MHz, $CDCl_3$) δ 194.16, 132.17, 129.89, 128.65, 127.44, 52.15, 45.08; HRMS (EI, 70 eV) calcd for C_9H_9ClO 168.0342, found 168.0347.

Determination of Mandelamide Hydrolase Activity. The mandelamide hydrolase activity was determined at 30 °C in 100 mM potassium phosphate buffer (pH 7.8) containing 1 mM EDTA. The release of ammonia from amide substrates was followed using a modification of the phenol and hypochlorite method of Krallmann-Wenzel (*34*). A reaction volume of 5 mL was used, and at appropriate time intervals 0.5 mL aliquots were withdrawn. These were added to 50 μL of a catalyst solution (a 3:1 mixture of 2 mM $MnSO_4$ and acetone) and 1 mL of phenol reagent. A sodium hypochlorite solution containing 1.5 g of free chlorine (0.5 mL)/100 mL was added and the solution vortexed. After a waiting period of at least 10 min, the absorbance at 636 nm was measured. The amount of ammonia that was released was extrapolated from a calibration curve of ammonia in the range of 0−100 nmol/mL, and the assay mixture, without enzyme, served as a blank.

MAH activity was also measured by a coupled assay initially described by Boshoff and Mizrahi for the determination of pyrazinamidase activity (*35*). In this study, the reaction mixture consisted of 100 mM potassium phosphate buffer (pH 7.8), 1 mM EDTA, 800 μM α-ketoglutarate, 200 μM NADPH, 15 units/mL L-glutamate dehydrogenase, and appropriate concentrations of amide in a final volume of 1 mL. After equilibration at 30 °C, the reaction was initiated by the addition of MAH. The decrease in the absorbance at 340 nm was monitored, and the rate of the reaction was determined using a molar extinction coefficient of 6220 M^{-1} cm^{-1} for reduced NADP.

Assays were carried out in triplicate (at least), and kinetic parameters were calculated by fitting to the Michaelis−Menten equation using nonlinear regression analysis.

pH Optimum. The optimal pH for MAH was determined in the constant-ionic strength buffer containing 100 mM MES, 50 mM diethanolamine, and 50 mM *N*-ethylmorpholine (*36*). A pH range of 5.0−9.0 was used, with 0.1 mM (*R*)-mandelamide as the substrate. MAH activity at 30 °C was measured by the coupled assay method. Assays were performed in duplicate.

Measurement of Esterase Activity. The esterase activity of MAH was determined by a pH-stat method using a TIM900 Titration Manager (Radiometer Analytical). The reaction mixture was comprised of the appropriate substrate (0.05−2.0 mM) and BSA (1 mg/mL) in a final volume of 3 mL. Following initiation of the reaction by the addition of MAH (1 μg/mL), the reaction mixture was titrated against 10 mM NaOH for 5 min using an end point pH of 8.5. Assays were performed in triplicate, at least.

Hydrolysis of N-Alkyl Phenylacetamides. Reactions were performed in 100 mM potassium phosphate at pH 7.5 and 30 °C. The assay mixture contained phenazine ethosulfate (4.8 mM), 2,6-dichlorophenolindophenol (170 μM), methylamine dehydrogenase (16 nM), and varied concentrations of substrates. The reaction was initiated by the addition of MAH and was monitored at 600 nm to determine the rate of reduction of dichlorophenolindophenol (*37*). Complete hydrolysis of *N*-methyl phenylacetamide, and lack of reaction with *N*-ethyl phenylacetamide, was demonstrated by initially incubating both substrates with high concentrations of MAH for an extended period of time (>24 h). An aliquot of each reaction mixture was then assayed with methylamine dehydrogenase. The extent of hydrolysis of *N*-methyl phenylacetamide and *N*-ethyl phenylacetamide was determined by extrapolation from a standard curve of methylamine and ethylamine, respectively.

Inhibition Studies. Reversible inhibition was examined using the coupled assay and appropriate concentrations of

Table 1: Kinetic Properties of Mandelamide Hydrolase with (*R*)- and (*S*)-Mandelamide[a]

	(*R*)-mandelamide			(*S*)-mandelamide		
enzyme	K_m (μM)	k_{cat} (s^{-1})	k_{cat}/K_m (M^{-1} s^{-1})	K_m (μM)	k_{cat} (s^{-1})	k_{cat}/K_m (M^{-1} s^{-1})
WT[b]	33.1 ± 1.0	15.7 ± 0.7	4.75×10^5	19.9 ± 3.3	9.0 ± 0.5	4.53×10^5
WT-his[b]	38.8 ± 1.7	20.7 ± 1.0	5.33×10^5	18.5 ± 2.9	10.0 ± 0.4	5.42×10^5
WT-his[c]	30.6 ± 3.4	26.4 ± 1.3	8.62×10^5	20.2 ± 2.2	10.5 ± 0.3	5.22×10^5

[a] Reactions were carried out at 30 °C in 100 mM potassium phosphate buffer (pH 7.8). The values represent the means of at least three individual experiments. [b] Determined using the phenol and hypochlorite method. [c] Determined using the coupled assay.

inhibitor and (*R*)-mandelamide. Reactions were initiated by the addition of MAH, and K_i values were determined using the method of Dixon (*38*). Evidence for time-dependent inhibition was sought in two ways. In the first instance, the enzyme was preincubated with the inhibitor and other components of the coupled assay for 15 or 30 min. The reaction was then initiated by the addition of substrate. In the second method, the enzyme was incubated with either the inhibitor or PMSF at 30 °C in 50 mM potassium phosphate (pH 7.8) in a total volume of 100 μL. At appropriate time intervals up to 60 min, an aliquot (20 μL) of this mixture was withdrawn and diluted 50-fold into the standard coupled assay mixture for analysis. For control reactions, the enzyme was preincubated for the same time intervals in the absence of the inhibitor. Again, aliquots (20 μL) were withdrawn and added to a standard assay mixture which contained either no inhibitor or an appropriate 50-fold dilution of the inhibitor.

RESULTS

Purification of MAH. Wild-type MAH was purified using a combination of ammonium sulfate fractionation, gel filtration, and ion-exchange chromatography. SDS−PAGE analysis indicated that the protein was >98% homogeneous with an apparent molecular mass of 54 kDa (data not shown). This method was time-consuming and somewhat cumbersome, requiring several dialysis steps, and so the possibility of using a C-terminal histidine tag was explored. This proved to be successful, and the His-tagged enzyme (MAH-his) could be purified to homogeneity (as evidenced by SDS−PAGE) in two steps with a yield of ca. 75 mg/L of culture. Mass spectrometric analysis provided molecular masses of 53 824 and 54 746 Da for MAH and MAH-his, respectively, which are in good agreement (±0.01%) with the calculated molecular masses of 53 817 and 54 751 Da, respectively (data not shown).

Enzyme Stability and Optimum pH. The purified enzyme, stored in potassium phosphate buffer (100 mM, pH 7.8) containing EDTA (1 mM), showed no detectable loss of activity at 4 °C for more than 1 month. Enzyme activity was maintained after several freeze (−20 °C) and thaw cycles. The pH optimum, determined in the constant-ionic strength buffer of Ellis and Morrison (*36*), was between 7.4 and 8.2. This is consistent with the pH optima obtained for other members of the AS family (*39*, *40*). A maximum was observed at pH 7.8, and this pH was used in later kinetic studies.

Catalytic Properties of MAH. The kinetic parameters, k_{cat} and K_m, for the MAH-catalyzed hydrolysis of (*R*)- and (*S*)-mandelamide are listed in Table 1. No significant differences in kinetic constants were observed between the wild-type and His-tagged enzymes for either substrate, indicating that the addition of the six histidine residues at the carboxy terminus did not affect the overall catalytic properties of the enzyme. The k_{cat} values for MAH-his were slightly higher for both substrates, probably reflecting its more rapid and efficient purification.

Generally, the activities of amidases have been measured using discontinuous assays such as the radiochemical assay used for FAAH (*19*, *41*) or the hydroxamate-based assay used for MAE2 (*26*, *42*). Our initial attempts to monitor ammonia release by reaction with indophenol (*43*) suggested that the method was not sufficiently sensitive, and so an assay based on the phenol and hypochlorite procedure of Krallmann-Wenzel (*34*) was developed. While this assay provided acceptable results (Table 1), a coupled assay, using L-glutamate dehydrogenase (*35*), was later found to provide more consistent data. The results obtained using the two assays are broadly similar (Table 1), although the k_{cat} for (*R*)-mandelamide was found to be slightly higher in the continuous assay. Unless otherwise stated, MAH-his and the coupled assay were used for all subsequent kinetic analyses.

Overall, both (*R*)- and (*S*)-mandelamide proved to be excellent substrates for MAH, with K_m values in the low micromolar range (Table 1). The values of K_m and k_{cat} for (*R*)-mandelamide were both higher than those for (*S*)-mandelamide, but the similar values of k_{cat}/K_m indicated that the enzyme was not enantioselective.

Substrate Specificity. Kinetic data for a range of substrates are given in Table 2. The value of k_{cat}/K_m for phenylacetamide was severalfold higher than for the 2-hydroxy derivatives. However, this was essentially related to substrate binding as the K_m value for phenylacetamide was at least 5-fold lower than the value for either (*R*)- or (*S*)-mandelamide while the k_{cat} values were all similar. There does appear to be a limit on the bulk tolerated at the 2 position as the 2-methoxy-substituted phenylacetamide shows a 10-fold increase in K_m and a 10-fold decrease in k_{cat}. The two-carbon side chain appears to be optimal as lengthening it (3-phenyl propionamide) leads to a more than 1000-fold reduction in k_{cat}/K_m. Benzamide, with the shorter side chain, was inactive as a substrate, although inhibition studies did indicate that it bound to the enzyme with a K_i value of 340 μM.

Given the apparent similarities to FAAH, a series of aliphatic substrates was also examined. Replacing the phenyl substituent with a methyl group (lactamide) led to greatly diminished (albeit measurable) activity. Hexanoamide and lauramide, with 6 and 12 carbon side chains, respectively, were also found to be substrates with values of k_{cat}/K_m comparable to that of 3-phenyl propionamide. The K_m value for hexanoamide (288 μM) was ~10-fold greater than that for (*R*)-mandelamide, while the K_m value for lauramide could not be determined as the substrate precipitated at concentrations of >150 μM. Surprisingly, stearamide with an 18-

Table 2: Kinetic Characterization of MAH with Alternative Substrates[a]

substrate	K_m (μM)	k_{cat} (s^{-1})	k_{cat}/K_m (M^{-1} s^{-1})	K_i[b] (μM)
benzamide	nad[c]	nad[c]	nad[c]	340
2-phenylacetamide	3.8 ± 0.1	14.2 ± 0.2	3.77×10^6	
3-phenylpropionamide	49 ± 4.1	0.12 ± 0.02	2.38×10^3	
(*R*)-2-methoxy-2-phenylacetamide	357 ± 19	1.73 ± 0.07	4.85×10^3	
N-methyl phenylacetamide[d]	32 ± 9.7	0.02 ± 0.002	6.98×10^2	
N-ethyl phenylacetamide[d]	nad[c]	nad[c]	nad[c]	
(*R*,*S*)-methyl mandelate[e]	170 ± 4	62.5 ± 2.2	3.68×10^5	
(*R*,*S*)-ethyl mandelate[e]	nad[c]	nad[c]	nad[c]	
lactamide	nd[f]	nd[f]	16.1 ± 0.6[g]	
hexanoamide	288 ± 24	0.48 ± 0.03	1.74×10^3	
lauramide (dodecanamide)	nd[f]	nd[f]	$(2.69 \pm 0.05) \times 10^3$[g]	
3-phenyl-1-chloro-2-propanone	–	–	–	130
3-phenyl-1,1,1-trifluoro-2-propanone	–	–	–	60

[a] Unless stated, determined using the coupled assay at 30 °C and pH 7.8. [b] Determined using Dixon plots. Errors are estimated to be ±10%. [c] No activity detected. [d] Determined using methylamine dehydrogenase as the coupling enzyme. [e] Determined using the pH-stat assay. [f] Not determined. [g] Determined using the coupled assay under V/K conditions.

Table 3: Summary of Kinetic Parameters for MAH Variants with (*R*)- and (*S*)-Mandelamide[a]

	(*R*)-mandelamide			(*S*)-mandelamide		
enzyme	K_m (μM)	k_{cat} (s^{-1})	k_{cat}/K_m (M^{-1} s^{-1})	K_m (μM)	k_{cat} (s^{-1})	k_{cat}/K_m (M^{-1} s^{-1})
WT	30.6 ± 3.4	26.4 ± 1.3	862000	20.2 ± 2.2	10.5 ± 0.3	522000
S180A	871 ± 19	0.018 ± 0.002	20.6	296 ± 25	0.007 ± 0.001	22.5
S181A	59 ± 7.2	0.018 ± 0.001	305	9.6 ± 0.6	0.007 ± 0.001	695
S204A	nad[b]	nad[b]	nad[b]	nad[b]	nad[b]	nad[b]
K100A	nad[b]	nad[b]	nad[b]	nad[b]	nad[b]	nad[b]

[a] Determined using the coupled assay as described in Experimental Procedures. [b] No activity detected.

carbon side chain also showed some evidence of hydrolysis, but its low solubility precluded the collection of meaningful kinetic data.

Some of the more intriguing results were obtained for N-substituted amides. Initially, it was thought that it would possible to assay the enzyme using 4′-nitromandelanilide as an alternative substrate. This would be expected to have two advantages in that the electron-withdrawing 4-nitrophenyl moiety would lower the pK_a of the leaving group, thereby accelerating the reaction (*44*), and that the reaction could be easily monitored by following the production of 4-nitroaniline at 382 nm. Anilides frequently serve as surrogate amides in mechanistic studies (*45*) and were used for FAAH (*20*), but unfortunately, MAH exhibited no reactivity with 4′-nitromandelanilide. Attention then turned to the *N*-methyl and *N*-ethyl derivatives of phenylacetamide. These could be assayed by coupling to methylamine dehydrogenase which is able to oxidize both methylamine and ethylamine (*37*). In this instance, hydrolysis of the *N*-methyl phenylacetamide was observed, albeit with a 5000-fold decrease in k_{cat}/K_m. No hydrolysis of the *N*-ethyl derivative was observed even after reaction for more than 24 h at high MAH concentrations. On the basis of these results, it appears that the active site of MAH will not accept anything larger than a methyl substituent on the amide nitrogen.

In hydrolysis reactions carried out in solution and using serine proteases, substrates are generally hydrolyzed with rate constants in the following order: ester > anilide > amide (*44*, *46*). FAAH has been reported to cleave esters and amides in a nonconventional manner (*20*), as reflected by its more rapid hydrolysis of amide than ester substrates (*9*, *20*, *21*), and even slower hydrolysis of a *p*-nitroanilide substrate (*20*). In this study, we find that (*R*,*S*)-methyl mandelate is hydrolyzed with a k_{cat} value that is ~3-fold greater than the value for (*R*)-mandelamide. However, the K_m value for methyl mandelate is also higher, and overall, its value of k_{cat}/K_m is marginally lower than the values for (*R*)- and (*S*)-mandelamide and 10-fold lower than that for phenylacetamide. These results again indicate that this class of enzymes operates by an unusual mechanism. MAH exhibited no activity with ethyl mandelate, nor did it hydrolyze 4-nitrophenyl phenylacetate which may also have been a useful alternative substrate. The lack of reactivity with the latter two esters lends credence to the suggestion that MAH will only tolerate limited steric bulk in its active site.

Serine proteases such as chymotrypsin have been characterized by their irreversible reaction with chloromethyl ketones (*46*, *47*). Preliminary studies showed that MAH could be inhibited by the serine-modifying agent phenylmethanesulfonyl fluoride (*48*). This was confirmed in the study presented here, with 1 mM PMSF leading to >80% inactivation within 1 h (data not shown). Consequently, it was thought that a chloromethyl ketone substrate analogue, such as 3-phenyl-1-chloro-2-propanone, may be useful as an affinity label. Although this compound proved to be a competitive inhibitor with a K_i value of 130 μM (Table 3), there was no evidence of time-dependent inhibition, and dilution studies indicated that binding was reversible (data not shown). Trifluoromethyl ketones have been used to inhibit FAAH (*49*, *50*) and are also used as slow-binding inhibitors of serine proteases (*51*) and esterases (*52*). 3-Phenyl-1,1,1-trifluoro-2-propanone is an analogue of phenylacetamide which binds even more tightly to MAH than 3-phenyl-1-chloro-2-propanone, having a K_i value of 60 μM. However, there was no evidence of slow onset inhibition.

Characterization of MAH Variants. Sequence alignments suggest that MAH was a member of the amidase superfamily (*7*). Members of this family are characterized by the presence

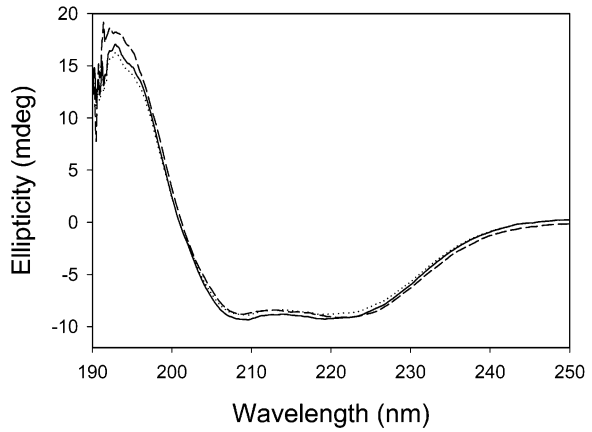

FIGURE 3: Far-UV circular dichroism spectra of MAH, MAH-his, and the K100A variant. The spectra for MAH (—), MAH-his (···), and K100A (− − −) were essentially identical to those of S180A, S181A, and S204A, which are not shown for the sake of clarity.

of the "amidase signature" which contains a GGSSXG motif as well as an invariant serine residue located 21 amino acids toward the C-terminus (Figure 2). In addition, there is a conserved lysine residue located some 80 residues toward the N-terminus. X-ray structures are now available for three members of this family: fatty acid amide hydrolase (*23*), malonamidase E2 (*8*, *22*), and peptide amidase (*24*). Although the structures suggest the presence of a novel Ser-*cis*-Ser-Lys catalytic triad, the importance of each of these residues has been assessed only for FAAH (*19*, *20*). It seemed logical to carry out a similar analysis for MAH, and accordingly, the K100A, S180A, S181A, and S204A variants were prepared as His-tagged derivatives.

The expression and purification proceeded smoothly, using the same procedures that were used for the WT enzyme. Mass spectrometry was used to confirm the presence of each mutation (data not shown). Figure 3 shows a comparison of the far-UV CD spectra of wild-type and His-tagged MAH as well as that of the K100A variant. The similarity of these spectra as well as the spectra of the other variants (not shown) clearly indicates that no major structural perturbations arose from either the presence of the histidine tag or the individual mutations. In Table 3 are listed the kinetic constants for the reaction of each of those mutants with both (*R*)- and (*S*)-mandelamide. Neither the K100A nor the S204A mutant showed detectable catalytic activity. The lack of activity of the latter mutant was not surprising as the replacement of the homologous serine residue in FAAH (*19*), MAE2 (*8*), and PAM (*24*) also led to an inactive enzyme. Conversely, replacement of the homologous lysine residue only led to reduced activity in FAAH (*9*, *20*), but did result in a total loss of activity in MAE2 (*8*).

Initial experiments with FAAH indicated that mutation of the two serines in the GGSSGG motif led to loss of activity in one instance and reduced activity in the other (*28*). More detailed studies showed that both S217A and S218A mutants possessed some amidase activity, although they were reduced by 2300- and 95-fold, respectively, from that of the WT enzyme (*19*). Their K_m values were relatively unaffected. The results in Table 3 show that replacement of either Ser180 or Ser181 with alanine resulted in a significant (~1500-fold) decrease in the value of k_{cat} for both enantiomers of mandelamide. K_m values for the S181A variant were relatively unchanged, with a slight increase for the (*R*)-enantiomer and a slight decrease for the (*S*)-enantiomer. However, the K_m values for the S180A mutant were both significantly higher, with increases of 30- and 15-fold for the (*R*)- and (*S*)-enantiomers of mandelamide, respectively. Overall, the k_{cat}/K_m values were decreased by at least 3 orders of magnitude, with the greatest effect being observed for the S180A mutant. This is similar to the results obtained for FAAH and lends credence to the suggestion that, for FAAH, Ser217 is catalytically more important than Ser218 (*19*). Other less detailed analyses suggest that the k_{cat} value for the S131A variant of MAE2 has decreased by 1700-fold (*8*) while that for the S202A variant of PAM shows a 140-fold decrease (*24*). The former, in particular, is in broad agreement with our data for S180A.

DISCUSSION

The aims of this study were twofold in that we sought to demonstrate that mandelamide hydrolase was a member of (i) the mandelate pathway and (ii) a member of the amidase signature family of enzymes. Originally, the genes for the enzymes of the mandelate pathway were found clustered on the chromosome (*2*, *3*). Later, they were isolated on a 10.5 kb fragment of chromosomal DNA (*4*) which was also found to contain the *mdl*Y gene. The *mdl*Y gene product, which carried the amidase signature (AS) sequence (Figure 2), was isolated and shown to hydrolyze mandelamide. Given the proximity of the gene to those of other members of the mandelate pathway, we proposed that mandelamide hydrolase was probably a new member of the mandelate pathway, although definitive evidence was lacking (*5*). To explore this further, we have expressed and purified MAH as a C-terminal His-tagged variant, which exhibits kinetic properties identical to those of the WT enzyme.

Kinetic and structural characterizations of members of the AS family suggest that they operate by a novel catalytic mechanism which employs a Ser-*cis*-Ser-Lys catalytic triad (*8*, *21*−*24*, *31*). However, the residues involved in substrate recognition are not conserved, which permits a broad range of substrate specificities. By comparison with FAAH, which accepts a wide variation in both the fatty acid acyl chain (*53*) and amine of the amide (*54*), MAH has a narrower substrate specificity. Our results indicate that phenylacetamide is the optimal substrate (Table 2) as alterations in the length of the side chain lead to significant decreases in binding affinity and k_{cat}/K_m. MAH will accept aliphatic substrates, with medium (6−12 carbon) length side chains being optimal, but both the binding affinity and k_{cat} are greatly reduced. The proposed physiological substrates, (*R*)- and (*S*)-mandelamide, have a hydroxyl group at the 2 position but are also excellent substrates, with values of k_{cat}/K_m only 10-fold lower than that of phenylacetamide. Much of the decrease is in lowered binding affinity, as the values of k_{cat} for all three compounds are quite similar. Interestingly, MAH does not appear to be greatly enantiomer specific. Several members of the AS family, including amidases from a *Rhodococcus* strain (*6*), *Brevibacterium* sp. strain R312 (*55*), *Rhodococcus erythropolis* MP50 (*56*, *57*), and *Agrobacterium tumefaciens* strain D3 (*58*), are able to hydrolyze a variety of aliphatic and aromatic amides with enantiomeric excesses of >99%. The values of k_{cat}/K_m for the reaction of MAH with (*R*)- and (*S*)-mandelamide are essentially identical,

although the (*S*)-enantiomer has a 2-fold lower value of K_m. This is more in line with results obtained for FAAH, for which the K_m value for (*R*)-α-methanandamide was 4-fold greater than the value for (*S*)-α-methanandamide, yet the V_{max} values were similar (*54*). It should also be noted that the binding pocket for the hydroxyl substituent of (*R*)-mandelamide must be relatively small as the (*R*)-2-methoxy-2-phenylacetamide has a 10-fold higher K_m value and a 10-fold lower k_{cat} value.

One surprising observation was that MAH tolerated very little substitution on the amide nitrogen. Initially, this was shown by the lack of reaction with mandelyl *p*-nitroanilide, which was somewhat surprising as this derivative had been used successfully in studies on FAAH (*20*) and EstA8, an AS family member from *Acinetobacter* (*39*). The *N*-ethyl derivative was also not tolerated; in fact, the only permitted variation was the *N*-methyl derivative which exhibited a 5000-fold decrease in k_{cat}/K_m. This decrease had contributions from an 8-fold increase in K_m and a 600-fold decrease in k_{cat}. Given that the base-catalyzed hydrolysis of acetamide was only 5-fold faster than that of *N*-methylacetamide and 10-fold faster than that of *N*-ethylacetamide (*59*), it is rather surprising to see the large differences in the k_{cat} values for phenylacetamide and *N*-methyl phenylacetamide. This is in marked contrast to FAAH which will accept an assortment of substituents on the amide nitrogen (*54*). Overall, these results suggest that, for MAH, the binding pocket for the amide group must be singularly small, and the substrate aligned precisely for efficient catalysis. Given that the vast majority of amide hydrolases are promiscuous, accepting a variety of amide substituents, it will be of interest to establish how MAH imposes such abnormally rigid constraints. We are hopeful our ongoing crystallographic studies will shed some light on this subject.

Previous studies have shown that MAH can be used to support growth of *P. putida* ATCC 17453 on (*R*,*S*)-mandelamide, but unlike other enzymes in the mandelate pathway, enzyme activity is not greatly induced by (*R*,*S*)-mandelate (*5*). The presence of mandelate racemase ensures that the lack of enantiospecificity of MAH is not a problem for later metabolism by (*S*)-mandelate dehydrogenase (Figure 1). Given that phenylacetamide is rarely found in metabolic processes, although it can be used as a sole carbon source by some *Pseudomonas aeruginosa* species (*60*), it is more likely that mandelamide is the physiological substrate for MAH. On that basis we maintain our conviction that MAH is indeed a member of the mandelate (now mandelamide?) pathway.

Sequence alignments suggested that the catalytic triad for MAH would comprise residues Ser180, Ser204, and Lys100. This proved to be the case as mutagenesis of any of these residues provided an enzyme with either no activity or severely impaired catalytic activity. The decrease in activity broadly mirrored results for FAAH (*19*, *21*, *28*), MAE2 (*8*), and PAM (*24*). Of particular note was the lack of activity with the K100A mutant with either amide or ester substrates. In FAAH, the analogous variant retained very little (<0.005%) residual activity with amide substrates and ca. 5% activity with ester substrates (*21*). By contrast, the K62A variant of MAE2 (*8*) and the K123A variant of PAM (*24*) showed no detectable amidase activity. It is conceivable that activity is observed only for the lysine mutant of FAAH because the radioactivity assay used for FAAH is more sensitive than the spectrophotometric assays used for MAH, MAE2, and PAM. However, as shown in Table 2, the MAH assay permits us to determine a value of k_{cat}/K_m for lactamide that is <0.0005% of the k_{cat}/K_m value for phenylacetamide. Further, the pH-stat assay used for esterase activity is sufficiently sensitive to observe a 1000-fold decrease in activity, which is certainly sufficient to detect the 5% residual activity seen for the FAAH K142A mutant. It should be noted that X-ray analysis showed that mutation of Lys62 to alanine led to a complete disruption of the MAE2 active site (*8*). If that were true for MAH, then the lack of activity with the K100A variant is not unexpected.

The role of the lysine residue in catalysis by amidase signature enzymes is somewhat contentious. For example, mechanisms proposed for both PAM (*24*) and MAE2 (*8*) require the lysine residue to be protonated, thus acting as an acid catalyst. Conversely, it is suggested that the lysine in FAAH is uncharged, and that it initiates the reaction by accepting a proton from Ser217, thus acting as a base catalyst (*21*). In a concerted reaction, a proton is then transferred to the substrate leaving group. In FAAH, this has the unusual effect of esters being hydrolyzed at the same rate as amides. Replacement of the lysine with alanine results in >100-fold lower rates of hydrolysis for amides than esters (*20*, *21*). Unfortunately, there are no detailed kinetic studies on either MAE2 or PAM which compare rates of ester and amide hydrolysis. Interestingly, EstA8 hydrolyzes *p*-nitrophenyl acetate ~100 times faster than *p*-nitrophenylacetanilide (*39*), suggesting that the behavior of FAAH is not necessarily typical of all AS enzymes. MAH seems to have kinetic properties similar to those of FAAH in that the k_{cat}/K_m values for the hydrolysis of (*R*,*S*)-methyl mandelate and the mandelamide enantiomers are similar. If anything, the catalytic efficiency with the ester substrate is slightly lower. It is difficult to assess individual effects on K_m and k_{cat} as the K_m values for esters are ~10-fold higher than those of their amide counterpart. However, at best, the value of k_{cat} for hydrolysis of methyl mandelate is only ~5-fold greater than that of mandelamide, clearly not the 2−3 orders of magnitude that may reasonably have been expected. It has been suggested that FAAH reacts with amide and ester substrates in predominantly acylation, or mixed acylation and deacylation, rate-limited reactions (*20*). Whether a similar mechanism is also in operation for MAH is the subject of further investigation.

One other notable difference between members of the amidase signature family is their reactivity with reagents such as phenylmethanesulfonyl fluoride (PMSF) and diisopropyl fluorophosphate (DFP) which generally (*61*), but not always (*62*), label the active site serine of serine proteases. These reagents had little or no effect on PAM (*24*), MAE2 (*26*), or the amidase from *Rhodococcus* J1 (*27*). Conversely, EstA8 was inhibited by low levels of PMSF (*39*), while FAAH was inhibited by both generic serine reagents (*49*), as well as more specific derivatives such as methyl arachidonyl fluorophosphonate (*63*) and ethoxy oleoyl fluorophosphonate (*19*). The differences in reactivity of the serine nucleophiles in PAM and FAAH were attributed to differences in the protonation state of the lysine residue. In FAAH, the lysine is thought to be unprotonated, and is able to participate in the activation of the serine nucleophile. Conversely, in PAM

and, by extension, MAE2, the protonated lysine is unable to assist, and the serine nucleophile is relatively deactivated.

MAH was readily inactivated by 1 mM PMSF, suggesting that the serine is relatively nucleophilic. However, unlike many serine proteases, MAH was not irreversibly inactivated by a chloromethyl ketone substrate analogue, even though it bound reasonably tightly. FAAH also displayed similar reactivity with PMSF and, like MAH, was not irreversibly inactivated by halomethyl ketones (*64*). Other inhibitors of serine proteases include peptidyl aldehydes such as chymostatin (*65*), boronic acids (*66*), and trifluoromethyl ketones (*67*). Chymostatin, which has been shown to inhibit PAM, is thought to act via initial formation of an encounter complex and subsequent attack of the active site serine to form a hemiacetal (*65*). Surprisingly, the X-ray structure of the PAM−chymostatin complex showed no evidence of covalent binding to the inhibitor (*24*), providing further support for the suggestion that the serine nucleophile in PAM is deactivated. A stable hemiketal adduct formed by attack of the nucleophilic serine on the electrophilic ketone group is thought to be the basis of inhibition by trifluoromethyl ketones (*68*). In some cases, this can lead to slow-binding inhibition (*51*, *69*). On the basis of the reactivity of MAH with PMSF, it was conceivable that MAH would also be inhibited by a trifluoromethyl ketone, potentially in a time-dependent manner. Not unexpectedly, the phenylacetamide analogue, 3-phenyl-1,1,1-trifluoro-2-propanone, was found to be a reversible inhibitor of MAH, with a K_i value of 60 μM. However, there was no evidence of time-dependent inhibition. Trifluoromethyl ketones were also used to probe the FAAH binding site (*70*) without any report of slow-binding behavior.

In summary, the results described herein reinforce our suggestion that mandelamide hydrolase represents an extension of the mandelate pathway. Further, it would seem that mandelamide hydrolase is a *bona fide* member of the amidase signature family. Its kinetic properties are, generally, more akin to those of fatty acid amide hydrolase than those of PAM and malonamidase E2. Our results lend support to the proposal that there are at least two groups of enzymes within the AS family and, potentially, that these groups employ different catalytic mechanisms.

ACKNOWLEDGMENT

We thank Prof. Victor Davidson and Limei H. Jones (University of Mississippi Medical Center) for providing us with methylamine dehydrogenase and assistance with setting up the MADH-coupled assay. We also thank Dr. Pan-Fen Wang for his help with obtaining the mass spectra of the MAH variants.

REFERENCES

1. Fewson, C. A. (1988) Microbial metabolism of mandelate: a microcosm of diversity, *FEMS Microbiol. Rev. 4*, 85−110.
2. Wheelis, M. L., and Stanier, R. Y. (1970) The genetic control of dissimilatory pathways in *Pseudomonas putida*, *Genetics 66*, 245−266.
3. Tsou, A. Y., Ransom, S. C., Gerlt, J. A., Powers, V. M., and Kenyon, G. L. (1989) Selection and characterization of a mutant of the cloned gene for mandelate racemase that confers resistance to an affinity label by greatly enhanced production of enzyme, *Biochemistry 28*, 969−975.
4. Tsou, A. Y., Ransom, S. C., Gerlt, J. A., Buechter, D. D., Babbitt, P. C., and Kenyon, G. L. (1990) Mandelate pathway of *Pseudomonas putida*: sequence relationship involving mandelate racemase, (*S*)-mandelate dehydrogenase, and benzoylformate decarboxylase and expression of benzoylformate decarboxylase in *Escherichia coli*, *Biochemistry 29*, 9856−9862.
5. McLeish, M. J., Kneen, M. M., Gopalakrishna, K. N., Koo, C. W., Babbitt, P. C., Gerlt, J. A., and Kenyon, G. L. (2003) Identification and characterization of a mandelamide hydrolase and an NAD(P)$^+$-dependent benzaldehyde dehydrogenase from *Pseudomonas putida* ATCC 12633, *J. Bacteriol. 185*, 2451−2456.
6. Mayaux, J. F., Cerbelaud, E., Soubrier, F., Yeh, P., Blanche, F., and Petre, D. (1991) Purification, cloning, and primary structure of a new enantiomer-selective amidase from a *Rhodococcus* strain: structural evidence for a conserved genetic coupling with nitrile hydratase, *J. Bacteriol. 173*, 6694−6704.
7. Chebrou, H., Bigey, F., Arnaud, A., and Galzy, P. (1996) Study of the amidase signature group, *Biochim. Biophys. Acta 1298*, 285−293.
8. Shin, S., Yun, Y. S., Koo, H. M., Kim, Y. S., Choi, K. Y., and Oh, B. H. (2003) Characterization of a novel Ser-cisSer-Lys catalytic triad in comparison with the classical Ser-His-Asp triad, *J. Biol. Chem. 278*, 24937−24943.
9. Patricelli, M. P., and Cravatt, B. F. (2000) Clarifying the catalytic roles of conserved residues in the amidase signature family, *J. Biol. Chem. 275*, 19177−19184.
10. Mazumder, A., Gerlt, J. A., Absalon, M. J., Stubbe, J., Cunningham, R. P., Withka, J., and Bolton, P. H. (1991) Stereochemical studies of the β-elimination reactions at aldehydic abasic sites in DNA: endonuclease III from *Escherichia coli*, sodium hydroxide, and Lys-Trp-Lys, *Biochemistry 30*, 1119−1126.
11. Gomi, K., Kitamoto, K., and Kumagai, C. (1991) Cloning and molecular characterization of the acetamidase-encoding gene (*amd*S) from *Aspergillus oryzae*, *Gene 108*, 91−98.
12. Gaffney, T. D., da Costa e Silva, O., Yamada, T., and Kosuge, T. (1990) Indoleacetic acid operon of *Pseudomonas syringae* subsp. savastanoi: transcription analysis and promoter identification, *J. Bacteriol. 172*, 5593−5601.
13. Deutsch, D. G., and Chin, S. A. (1993) Enzymatic synthesis and degradation of anandamide, a cannabinoid receptor agonist, *Biochem. Pharmacol. 46*, 791−796.
14. Cravatt, B. F., Giang, D. K., Mayfield, S. P., Boger, D. L., Lerner, R. A., and Gilula, N. B. (1996) Molecular characterization of an enzyme that degrades neuromodulatory fatty-acid amides, *Nature 384*, 83−87.
15. Curnow, A. W., Hong, K., Yuan, R., Kim, S., Martins, O., Winkler, W., Henkin, T. M., and Soll, D. (1997) Glu-tRNAGln amidotransferase: a novel heterotrimeric enzyme required for correct decoding of glutamine codons during translation, *Proc. Natl. Acad. Sci. U.S.A. 94*, 11819−11826.
16. Schon, A., Kannangara, C. G., Gough, S., and Soll, D. (1988) Protein biosynthesis in organelles requires misaminoacylation of tRNA, *Nature 331*, 187−190.
17. Fowler, C. J., Jonsson, K. O., and Tiger, G. (2001) Fatty acid amide hydrolase: biochemistry, pharmacology, and therapeutic possibilities for an enzyme hydrolyzing anandamide, 2-arachidonoylglycerol, palmitoylethanolamide, and oleamide, *Biochem. Pharmacol. 62*, 517−526.
18. Boger, D. L., Sato, H., Lerner, A. E., Hedrick, M. P., Fecik, R. A., Miyauchi, H., Wilkie, G. D., Austin, B. J., Patricelli, M. P., and Cravatt, B. F. (2000) Exceptionally potent inhibitors of fatty acid amide hydrolase: the enzyme responsible for degradation of endogenous oleamide and anandamide, *Proc. Natl. Acad. Sci. U.S.A. 97*, 5044−5049.
19. Patricelli, M. P., Lovato, M. A., and Cravatt, B. F. (1999) Chemical and mutagenic investigations of fatty acid amide hydrolase: evidence for a family of serine hydrolases with distinct catalytic properties, *Biochemistry 38*, 9804−9812.
20. Patricelli, M. P., and Cravatt, B. F. (1999) Fatty acid amide hydrolase competitively degrades bioactive amides and esters through a nonconventional catalytic mechanism, *Biochemistry 38*, 14125−14130.
21. McKinney, M. K., and Cravatt, B. F. (2003) Evidence for distinct roles in catalysis for residues of the serine-serine-lysine catalytic triad of fatty acid amide hydrolase, *J. Biol. Chem. 278*, 37393−37399.
22. Shin, S., Lee, T. H., Ha, N. C., Koo, H. M., Kim, S. Y., Lee, H. S., Kim, Y. S., and Oh, B. H. (2002) Structure of malonamidase

E2 reveals a novel Ser-*cis*Ser-Lys catalytic triad in a new serine hydrolase fold that is prevalent in nature, *EMBO J. 21*, 2509−2516.
23. Bracey, M. H., Hanson, M. A., Masuda, K. R., Stevens, R. C., and Cravatt, B. F. (2002) Structural adaptations in a membrane enzyme that terminates endocannabinoid signaling, *Science 298*, 1793−1796.
24. Labahn, J., Neumann, S., Buldt, G., Kula, M. R., and Granzin, J. (2002) An alternative mechanism for amidase signature enzymes, *J. Mol. Biol. 322*, 1053−1064.
25. Murzin, A. G., Brenner, S. E., Hubbard, T., and Chothia, C. (1995) SCOP: a structural classification of proteins database for the investigation of sequences and structures, *J. Mol. Biol. 247*, 536−540.
26. Koo, H. M., Choi, S. O., Kim, H. M., and Kim, Y. S. (2000) Identification of active-site residues in *Bradyrhizobium japonicum* malonamidase E2, *Biochem. J. 349*, 501−507.
27. Kobayashi, M., Fujiwara, Y., Goda, M., Komeda, H., and Shimizu, S. (1997) Identification of active sites in amidase: evolutionary relationship between amide bond- and peptide bond-cleaving enzymes, *Proc. Natl. Acad. Sci. U.S.A. 94*, 11986−11991.
28. Omeir, R. L., Arreaza, G., and Deutsch, D. G. (1999) Identification of two serine residues involved in catalysis by fatty acid amide hydrolase, *Biochem. Biophys. Res. Commun. 264*, 316−320.
29. Audrieth, L. F., and Sveda, M. (1955) Mandelamide, in *Organic Syntheses* (Horning, E. C., Ed.) Collect. Vol. III, pp 536−538, Wiley & Sons, New York.
30. *Dictionary of Organic Compounds*, 6th ed. (1996) Vol. 4, p 3790, Chapman & Hall, London.
31. Bailén, M. A., Chinchilla, R., Dodsworth, D. J., and Nájera, C. (2000) Efficient synthesis of primary amides using 2-mercaptopyridone-1-oxide-based uronium salts, *Tetrahedron Lett. 41*, 9809−9813.
32. Bovin, J., El Kaim, L., and Zard, S. Z. (1995) A New and Efficient Synthesis of Trifluoromethyl Ketones from Carboxylic Acids. Part I, *Tetrahedron 51*, 2573−2584.
33. McPhee, W. D., and Klingsberg, E. (1955) Benzyl chloromethyl ketone, In *Organic Syntheses* (Horning, E. C., Ed.) Collect. Vol. 3, pp 119−200, Wiley & Sons, New York.
34. Krallmann-Wenzel, U. (1985) An improved method of ammonia determination, applicable to amidases and other ammonia-producing enzyme systems of mycobacteria, *Am. Rev. Respir. Dis. 131*, 432−434.
35. Boshoff, H. I., and Mizrahi, V. (1998) Purification, gene cloning, targeted knockout, overexpression, and biochemical characterization of the major pyrazinamidase from *Mycobacterium smegmatis*, *J. Bacteriol. 180*, 5809−5814.
36. Ellis, K. J., and Morrison, J. F. (1982) Buffers of constant ionic strength for studying pH-dependent processes, *Methods Enzymol. 87*, 405−426.
37. Zhu, Z., Sun, D., and Davidson, V. L. (2000) Conversion of methylamine dehydrogenase to a long-chain amine dehydrogenase by mutagenesis of a single residue, *Biochemistry 39*, 11184−11186.
38. Dixon, M. (1953) The determination of enzyme inhibitor constants, *Biochem. J. 55*, 170−171.
39. Wei, Y., Kurihara, T., Suzuki, T., and Esaki, N. (2003) A novel esterase from a psychrotrophic bacterium, *Acinetobacter* sp. strain no. 6, that belongs to the amidase signature family, *J. Mol. Catal. B: Enzym. 23*, 357−365.
40. Neumann, S., and Kula, M. R. (2002) Gene cloning, overexpression and biochemical characterization of the peptide amidase from *Stenotrophomonas maltophilia*, *Appl. Microbiol. Biotechnol. 58*, 772−780.
41. Patricelli, M. P., Lashuel, H. A., Giang, D. K., Kelly, J. W., and Cravatt, B. F. (1998) Comparative characterization of a wild type and transmembrane domain-deleted fatty acid amide hydrolase: identification of the transmembrane domain as a site for oligomerization, *Biochemistry 37*, 15177−15187.
42. Kim, Y. S., and Kang, S. W. (1994) Novel malonamidases in *Bradyrhizobium japonicum*. Purification, characterization, and immunological comparison, *J. Biol. Chem. 269*, 8014−8021.
43. Kaplan, A. (1969) The determination of urea, ammonia, and urease, *Methods Biochem. Anal. 17*, 311−324.
44. Hegazi, M. F., Quinn, D. M., and Schowen, R. L. (1978) Transition-state properties in acyl and methyl transfer, in *Transition States of Biochemical Processes* (Gandour, R. D., and Schowen, R. L., Eds.) pp 355−428, Plenum Press, New York.
45. Stein, R. L. (2002) Enzymatic hydrolysis of *p*-nitroacetanilide: mechanistic studies of the aryl acylamidase from *Pseudomonas fluorescens*, *Biochemistry 41*, 991−1000.
46. Walsh, C. T. (1979) *Enzymatic Reaction Mechanisms*, W. H. Freeman and Co., San Francisco.
47. Schoellmann, G., and Shaw, E. (1963) Direct evidence for the presence of histidine in the active center of chymotrypsin, *Biochemistry 2*, 252−255.
48. Koo, C. W. (1997) Mandelamide hydrolase from *Pseudomonas putida*, Ph.D. Thesis, Department of Pharmaceutical Chemistry, University of California, San Francisco.
49. Ueda, N., Kurahashi, Y., Yamamoto, S., and Tokunaga, T. (1995) Partial purification and characterization of the porcine brain enzyme hydrolyzing and synthesizing anandamide, *J. Biol. Chem. 270*, 23823−23827.
50. Koutek, B., Prestwich, G. D., Howlett, A. C., Chin, S. A., Salehani, D., Akhavan, N., and Deutsch, D. G. (1994) Inhibitors of arachidonoyl ethanolamide hydrolysis, *J. Biol. Chem. 269*, 22937−22940.
51. Stein, R. L., Strimpler, A. M., Edwards, P. D., Lewis, J. J., Mauger, R. C., Schwartz, J. A., Stein, M. M., Trainor, D. A., Wildonger, R. A., and Zottola, M. A. (1987) Mechanism of slow-binding inhibition of human leukocyte elastase by trifluoromethyl ketones, *Biochemistry 26*, 2682−2689.
52. Allen, K. N., and Abeles, R. H. (1989) Inhibition of pig liver esterase by trifluoromethyl ketones: modulators of the catalytic reaction alter inhibition kinetics, *Biochemistry 28*, 135−140.
53. Boger, D. L., Fecik, R. A., Patterson, J. E., Miyauchi, H., Patricelli, M. P., and Cravatt, B. F. (2000) Fatty acid amide hydrolase substrate specificity, *Bioorg. Med. Chem. Lett. 10*, 2613−2616.
54. Lang, W., Qin, C., Lin, S., Khanolkar, A. D., Goutopoulos, A., Fan, P., Abouzid, K., Meng, Z., Biegel, D., and Makriyannis, A. (1999) Substrate specificity and stereoselectivity of rat brain microsomal anandamide amidohydrolase, *J. Med. Chem. 42*, 896−902.
55. Mayaux, J. F., Cerebelaud, E., Soubrier, F., Faucher, D., and Petre, D. (1990) Purification, cloning, and primary structure of an enantiomer-selective amidase from *Brevibacterium sp.* strain R312: structural evidence for genetic coupling with nitrile hydratase, *J. Bacteriol. 172*, 6764−6773.
56. Hirrlinger, B., Stolz, A., and Knackmuss, H. J. (1996) Purification and properties of an amidase from *Rhodococcus erythropolis* MP50 which enantioselectively hydrolyzes 2-arylpropionamides, *J. Bacteriol. 178*, 3501−3507.
57. Trott, S., Burger, S., Calaminus, C., and Stolz, A. (2002) Cloning and heterologous expression of an enantioselective amidase from *Rhodococcus erythropolis* strain MP50, *Appl. Environ. Microbiol. 68*, 3279−3286.
58. Trott, S., Bauer, R., Knackmuss, H. J., and Stolz, A. (2001) Genetic and biochemical characterization of an enantioselective amidase from *Agrobacterium tumefaciens* strain d3, *Microbiology 147*, 1815−1824.
59. Yamana, T., Mizukami, Y., Tsuji, A., Yasuda, Y., and Masuda, K. (1972) Stability of amides. I. Hydrolysis mechanism of N-substituted aliphatic amides, *Chem. Pharm. Bull. 20*, 881−891.
60. Gregoriou, M., and Brown, P. R. (1980) Adaptation to phenylacetamide as a growth substrate by an acetanilide-utilizing mutant of *Pseudomonas aeruginosa*, *Arch. Microbiol. 125*, 277−283.
61. Carter, P., and Wells, J. A. (1988) Dissecting the catalytic triad of a serine protease, *Nature 332*, 564−568.
62. Zwizinski, C., Date, T., and Wickner, W. (1981) Leader peptidase is found in both the inner and outer membranes of *Escherichia coli*, *J. Biol. Chem. 256*, 3593−3597.
63. Deutsch, D. G., Omeir, R., Arreaza, G., Salehani, D., Prestwich, G. D., Huang, Z., and Howlett, A. (1997) Methyl arachidonyl fluorophosphonate: a potent irreversible inhibitor of anandamide amidase, *Biochem. Pharmacol. 53*, 255−260.
64. Patricelli, M. P., Patterson, J. E., Boger, D. L., and Cravatt, B. F. (1998) An endogenous sleep-inducing compound is a novel competitive inhibitor of fatty acid amide hydrolase, *Bioorg. Med. Chem. Lett. 8*, 613−618.
65. Stein, R. L., and Strimpler, A. M. (1987) Slow-binding inhibition of chymotrypsin and cathepsin G by the peptide aldehyde chymostatin, *Biochemistry 26*, 2611−2615.
66. Kettner, C. A., and Shenvi, A. B. (1984) Inhibition of the serine proteases leukocyte elastase, pancreatic elastase, cathepsin G, and

chymotrypsin by peptide boronic acids, *J. Biol. Chem. 259*, 15106−15114.
67. Imperiali, B., and Abeles, R. H. (1986) Inhibition of serine proteases by peptidyl fluoromethyl ketones, *Biochemistry 25*, 3760−3767.
68. Brady, K., Wei, A. Z., Ringe, D., and Abeles, R. H. (1990) Structure of chymotrypsin-trifluoromethyl ketone inhibitor complexes: comparison of slowly and rapidly equilibrating inhibitors, *Biochemistry 29*, 7600−7607.
69. Morrison, J. F., and Walsh, C. T. (1988) The behavior and significance of slow-binding enzyme inhibitors, *Adv. Enzymol. Relat. Areas Mol. Biol. 61*, 201−301.
70. Boger, D. L., Sato, H., Lerner, A. E., Austin, B. J., Patterson, J. E., Patricelli, M. P., and Cravatt, B. F. (1999) Trifluoromethyl ketone inhibitors of fatty acid amide hydrolase: a probe of structural and conformational features contributing to inhibition, *Bioorg. Med. Chem. Lett. 9*, 265−270.
71. Altschul, S. F., Madden, T. L., Schaffer, A. A., Zhang, J., Zhang, Z., Miller, W., and Lipman, D. J. (1997) Gapped BLAST and PSI-BLAST: a new generation of protein database search programs, *Nucleic Acids Res. 25*, 3389−3402.

BI049907Q